Jump phenomenon induced by potential strength variation and the influence of exotic resonant states

Cornelia Grama, N. Grama, and I. Zamfirescu
Horia Hulubei Institute of Physics and Nuclear Engineering, P.O. Box MG-6, Bucharest, Romania
(Received 10 May 2003; published 30 September 2003)

The jump phenomenon between two *S*-matrix poles induced by a small potential strength variation is studied in the framework of the nonrelativistic scattering by a central potential $gV(r)$, $g \in \mathrm{C}$. Let $R_g^{(l)}$ denote the Riemann surface over the complex g plane, on which the pole function $k=k^{(l)}(g)$ is single valued and analytic. By associating a sheet $\Sigma_n^{(l)}$ of $R_g^{(l)}$ and its k-plane image $\Sigma_n'^{(l)}$ to a state with the quantum numbers (l,n), the jump between the states (l,n) and (l,m), induced by the potential strength variation, is understood as the jump between the sheet images $\Sigma_n'^{(l)}$ and $\Sigma_m'^{(l)}$. The rules for the jumps $(l,n) \Leftrightarrow (l,m)$ as a consequence of a small potential strength variation are deduced. The influence of the exotic resonant states on the selection rules for the jumps is discussed. The occurrence of the local degeneracy with respect to l of the resonant levels $(l-1,n)$, (l,m), and $(l+1,p)$ for the rectangular central potential and the level stability with respect to the potential strength variation are also discussed.

DOI: 10.1103/PhysRevA.68.032723 PACS number(s): 03.65.Nk, 34.50.−s, 34.80.Bm

I. INTRODUCTION

We consider the nonrelativistic scattering of a spinless particle by a central potential $gV(r)$, $g \in C$. In a scattering problem the potential $gV(r)$ represents a mean potential. For example, in atomic physics it represents the mean intermolecular potential averaged over internal states. Consequently, the potential strength g could undergo small changes and we may ask which is the effect of these changes.

An adequate quantum-mechanical description of the bound and resonant states is through the *S*-matrix poles. The function $k=k^{(l)}(g)$ which defines a *S*-matrix bound- and resonant-state pole as a function of the potential strength g is a multivalued function. In Ref. [1] an approach to bound and resonant states, based on the construction of the Riemann surface over the g plane, on which the pole function $k=k^{(l)}(g)$ is single valued and analytic, has been presented. The Riemann surface $R_g^{(l)}$ has been divided into sheets $\Sigma_n^{(l)}$ and the images $\Sigma_n'^{(l)}$ of these sheets in the k plane have been constructed. If the potential strength g takes a value on a given sheet $\Sigma_n^{(l)}$, then the function $k=k^{(l)}(g)$ takes only one value on the k-plane image $\Sigma_n'^{(l)}$ of the sheet, i.e., there is only a single pole on each sheet image. In other words each branch of the function $k=k^{(l)}(g)$ is situated on the k-plane image of the associated Riemann sheet. In this way the sheet $\Sigma_n^{(l)}$ of the Riemann surface $R_g^{(l)}$ and its k-plane image $\Sigma_n'^{(l)}$ have been associated to a given state with quantum numbers (l,n). This allows us to study each state (l,n) separately and to understand the jump from the state (l,n) to the state (l,m) as a result of a small potential strength variation.

Let us suppose that the potential strength has a small variation around a branch point of the function $k=k^{(l)}(g)$. This small potential strength variation can either determine a small change of the pole function $k=k^{(l)}(g)$, or it may induce a large variation of the function $k=k^{(l)}(g)$ by the transition from one branch of the function to another branch. Variation of the parameter g can determine a transition from a quantitative change to a qualitative change, i.e., in a jump phenomenon. As jump phenomena, ubiquitous in science [2], are characterized by large dynamic responses of the system to small amplitude disturbances, it is justified to call "jump" the transition of the system from the state (l,n) to the state (l,m) as a result of a small potential strength variation. The rules governing the jump phenomenon are important in the study of the pole trajectories. In such a study the position of a pole in the k plane is investigated as a function of the potential strength. By knowing the jumping rules one avoids the accidental jumps from one pole to other pole when one calculates the pole trajectories. In this way we are sure that the same pole is followed.

The aim of this paper is to establish the conditions for the system to undergo a jump from one state (l,n) to other state (l,m) as a consequence of a small potential strength variation. Let the parameter g follow a prescribed contour starting from a value $g \in \Sigma_n^{(l)}$. The choice of the contour can induce quite distinct effects: (a) if g describes a closed curve on $\Sigma_n^{(l)}$ not enclosing a branch point where $\Sigma_n^{(l)}$ is joined to other sheet, then its image $k=k^{(l)}(g)$ takes values on a continuous path on the Riemann sheet image $\Sigma_n'^{(l)}$, i.e., the potential strength variation does not change the state (l,n); (b) on the contrary, if g describes a closed contour which starts from a point on the sheet $\Sigma_n^{(l)}$ and encloses the branch point joining the sheets $\Sigma_n^{(l)}$ and $\Sigma_m^{(l)}$ and no other branch points, then the variable g is transferred from the sheet $\Sigma_n^{(l)}$ to the sheet $\Sigma_m^{(l)}$. As a consequence, the pole $k=k^{(l)}(g)$ is transferred from the sheet image $\Sigma_n'^{(l)}$ to the sheet image $\Sigma_m'^{(l)}$. In other words the potential strength variation induces a jump from the state (l,n) to the state (l,m).

In the following a rectangular central potential

$$\frac{2mR^2}{\hbar^2} gV(r) = \begin{cases} -g & \text{for } r/R \leqslant 1, \quad g \in \mathbf{C}, \\ 0 & \text{for } r/R > 1, \end{cases} \tag{1}$$

will be considered. We will use the dimensionless variable

 ©2003 The American Physical Society

r/R rather than the variable r. For the sake of simplicity in the following, the notation k will be used for the dimensionless variable kR.

In order to understand the jumps between the states (l,n) and (l,m) or, equivalently, the jumps from the k-plane image of a sheet Σ_n of the Riemann surface $R_g^{(l)}$ to the k-plane image of other sheet Σ_m, the way the various sheets are joined at the branch points has to be analyzed. The Riemann surfaces for a large range of orbital angular-momentum values l have to be studied in order to extract a rule governing the jumps. In the present paper the range $l=0-8$ is covered. In Sec. II the jumps between the Riemann sheets of a Riemann surface $R_g^{(l)}$ for a given l are studied. In Ref. [1] it was shown that in the case of a potential well followed by a barrier, there were poles situated on certain Riemann sheet images that had extraordinary properties so that they have been called ''exotic'' poles. An exotic resonant-state pole does not become a bound- or virtual-state pole as the depth of the potential well increases to infinity, but it remains a resonant-state pole situated in the neighborhood of an attractor in the k plane. The wave function of the exotic resonant state corresponding to an exotic resonant pole situated near the attractor is almost completely localized inside the potential barrier. In Ref. [3] it was shown that for a potential made of a well plus a Coulomb barrier the exotic poles situated at certain attractors correspond to the well known quasimolecular states excited in heavy-ion collisions. The properties of the quasimolecular states [energies, widths, deviation from the linear dependence of the energy on $l(l+1)$, doorway character, and criteria for observability] have been shown to result naturally from the general properties of the exotic resonant states. The influence of the exotic resonant-state poles on the rules governing the jumps is discussed in Sec. II C.

Another effect produced by the potential strength variation is the occurrence of the local degeneracy of the resonant levels for the rectangular central potential with respect to the orbital angular momentum. Recently, the problem of multiple pole degeneracy for a given l has been discussed by several authors [4–9] for various potentials. In the present paper some other kind of pole degeneracy will be studied, namely, the degeneracy with respect to the orbital angular momentum. In Ref. [1] it was shown that three Riemann sheets belonging to three distinct Riemann surfaces $R_g^{(l-1)}$, $R_g^{(l)}$, and $R_g^{(l+1)}$ are joined at some special values of the potential strength. In other words three resonant levels $(l-1,n)$, (l,m), and $(l+1,p)$ are degenerate, provided that the potential strength takes a value from a given discrete set. The labels n, m, and p of the sheets of $R_g^{(l-1)}$, $R_g^{(l)}$, and $R_g^{(l+1)}$ that are joined at each of these special values of the potential strength, extracted by the analysis of the Riemann surfaces, are given in Sec. III. If the potential strength varies around one of these special values, the degeneracy of the three resonant states may be brought about and the cooperative contribution in the cross section from three adjacent partial waves occurs. The occurrence of the local degeneracy with respect to l as an effect of the potential strength variation and the level stability in the three adjacent waves $(l-1)$, l, and $(l+1)$ are discussed in Sec. III.

II. JUMPS BETWEEN STATES WITH THE SAME *l*

In the case of a central rectangular potential besides the logarithmic branch point $g=0$, where all the sheets $\Sigma_n^{(l)}$ are joined, there are the following algebraic branch points of the function $k=k^{(l)}(g)$:

$$g_{s,s'}^{l,+}=(\kappa_{0,s}^{l,+})^2-(\kappa_{s'}^{l,+})^2, \tag{2}$$

$$g_{s,s'}^{l,-}=(\kappa_{0,s}^{l,-})^2-(\kappa_{s'}^{l,-})^2, \quad l>1, \tag{3}$$

where $\kappa_{0,s}^{l,+}$ and $\kappa_{0,s}^{l,-}$ $(s=1,2,\ldots)$ are the zeros of the spherical Bessel functions $j_{l+1}(z)$ and $j_{l-1}(z)$, respectively. $\kappa_{s'}^{l,+}$ and $\kappa_{s'}^{l,-}$ are the zeros of the spherical Hankel functions of the first kind, i.e., $h_{l+1}^{(1)}(z)$ and $h_{l-1}^{(1)}(z)$, respectively. In Ref. [1] it was shown that all the branch points $g_{s,s'}^{l,\pm}$ are of order one, i.e., there are only two sheets that are joined at each algebraic branch point $g_{s,s'}^{l,\pm}$.

The k-plane images of the branch points $g_{s,s'}^{l,+}$ are the complex zeros of the spherical Hankel functions of the first kind, $h_{l+1}^{(1)}(z)$. Similarly the k-plane images of the branch points $g_{s,s'}^{l,-}$ are the complex zeros of the spherical Hankel functions of the first kind, $h_{l-1}^{(1)}(z)$. According to Ref. [10], $h_m^{(1)}(z)$ has m zeros situated along an half-eye shaped curve in the lower k half plane, symmetrically distributed with respect to the imaginary k axis. Due to the symmetry with respect to the imaginary k axis for a given even l, there are $l+1$ images of the branch points in the fourth quadrant of the k plane including the imaginary k axis, distributed on two half-eye shaped curves: $l/2$ zeros of $h_{l-1}^{(1)}(z)$ and $l/2+1$ zeros of $h_{l+1}^{(1)}(z)$. Similarly, for a given odd l in the fourth quadrant of the k plane, there are l images of the branch points, distributed on the two half-eye shaped curves: $(l-1)/2$ zeros of $h_{l-1}^{(1)}(z)$ and $(l+1)/2$ zeros of $h_{l+1}^{(1)}(z)$. The way the images of the branch points in the fourth quadrant of the k plane are denoted is illustrated in Fig. 1(a) for even l and Fig. 1(b) for odd l. There is an infinity of branch points $g_{s,s'}^{l,\pm}$ for a given s' that have the same k-plane image $\kappa_{s'}^{\pm}=k(g_{s,s'}^{l,\pm})$, as s takes an infinity of values $s=1,2,3,\ldots$.

In Ref. [1] a quantum number n with a topological meaning has been introduced in order to label the Riemann sheets and their k-plane images. Because there is a single pole on a given Riemann sheet image, the label n of the sheet image $\Sigma_n'^{(l)}$ is also used as a label for that pole and for the corresponding state (l,n). The integer n counts the roots of the pole equation for $g=0$ [see Eq. (3.17) of Ref. [1]]. The Riemann sheet analysis shows that there are two classes of resonant poles: (a) the class of usual resonant-state poles that have the familiar property to become bound- or virtual-state poles when the depth of the potential well is increased and (b) the class of exotic resonant-state poles that remain in bound regions of the lower k half plane, in the neighborhood of some attractors, when the potential strength of the well is

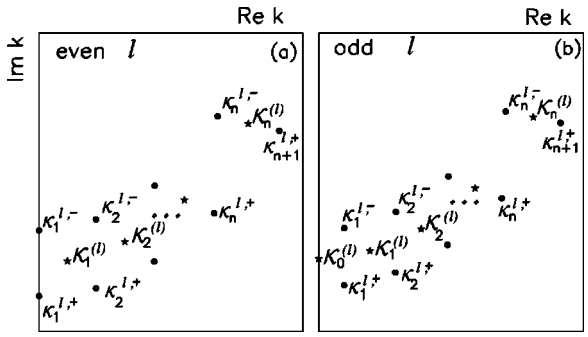

FIG. 1. In panels (a) and (b) the way the images $\kappa_{s'}^{l,\pm}$ of the branch points $g_{s,s'}^{l,\pm}$ are distributed in the fourth quadrant of the k plane for even l and for odd l, respectively, is schematically represented. By ● the images $k(g_{s,s'}^{l,\pm})=\kappa_{s'}^{l,\pm}$ of the branch points $g_{s,s'}^{l,\pm}$ that are the zeros of the spherical Hankel function of the first order, $h_{l\pm1}^{(1)}(z)$, are indicated. By ⋆ the attractors $\mathcal{K}_i^{(l)}$, which are the zeros of the spherical Hankel function of the first order, $h_l^{(1)}(z)$, are indicated. In the case of even l the images of the branch points $g_{s,1}^{l,-}$ and $g_{s,1}^{l,+}$ are situated on the negative imaginary k axis and the value of the label n is $n=l/2$. In the case of odd l the value of the label n is $n=(l-1)/2$.

increased. The exotic resonant state poles exist for $l\geqslant 1$, and they are located on certain Riemann sheet images.

Because at the logarithmic branch point $g=0$ all the Riemann sheets are joined together, in the following only the junctions at the algebraic branch points $g_{s,s'}^{l,\pm}$ will be studied. In order to establish which are the sheets that are joined at each algebraic branch point, $g_{s,s'}^{l,\pm}$, successive small circuits $|g-g_{s,s'}^{l,\pm}|=\rho$ are taken round the given branch point $g_{s,s'}^{l,\pm}$. Let us start with $g=g_i\in\Sigma_n^{(l)}$ and $k_i=k^{(l)}(g_i)\in\Sigma_n'^{(l)}$. After a complete rotation of g round the branch point, $g_{s,s'}^{l,\pm}$, the pole reaches the other value $k=k_f\in\Sigma_m'^{(l)}$. After a second complete rotation of g, the pole reaches again its initial value $k_i\in\Sigma_n'^{(l)}$. It results that $g_{s,s'}^{l,\pm}$ is a branch point where the sheets $\Sigma_n^{(l)}$ and $\Sigma_m^{(l)}$ are joined together. If the function $k=k^{(l)}(g)$ returns to its initial value after a complete rotation of g round $g_{s,s'}^{l,\pm}$, then $g_{s,s'}^{l,\pm}$ is not a branch point for $\Sigma_n^{(l)}$. The values of the first three branch points $g_{s,s'}^{l,\pm}$ (i.e., for $s=1,2,$ and 3) that have the images in the fourth quadrant of the k plane in the case $l=0-8$ are given in Table I. A similar table has been published in Ref. [1] for $l=0-4$. However, in the present paper the necessity to give some rules for the junctions imposes other labeling of the branch points. In comparison to Ref. [1] the labels are presently assigned in a more systematic way, as explained above and illustrated in Fig. 1.

The algebraic branch points are of order one, so that there are only two sheets that are joined at each $g_{s,s'}^{l,\pm}$. The rules that specify the labels n and m of the sheets that are joined at each branch point $g_{s,s'}^{l,\pm}$ (junction rules) can be established. The labels n and m of the sheets joined at a given $g_{s,s'}^{l,\pm}$ are determined by the procedure mentioned above. From the analysis of the Riemann surfaces some regularities concerning the junctions between the sheets of each $R_g^{(l)}$ at the branch points having the images in the fourth quadrant of the k plane and on the negative imaginary k axis have been observed. Rules for the junctions between the Riemann sheets are extracted and given in Secs. II A and II B. However, the existence of the exotic resonant-state poles on the sheet images $\Sigma_n'^{(l)}$ with $n=1,2,\ldots,l/2$ for even l and $n=0,1,\ldots,(l-1)/2$ for odd l induces some exceptions to the junction rules. If for the potential strength value $g_{s,s'}^{l,\pm}$ there are exotic resonant-state poles on $\Sigma_n'^{(l)}$ and $\Sigma_m'^{(l)}$ with $m>n$, then $g=g_{s,s'}^{l,\pm}$ is not a branch point where the sheets $\Sigma_n^{(l)}$ and $\Sigma_m^{(l)}$ are joined. The reason for this will be explained in Sec. II C. As a consequence, $\Sigma_n^{(l)}$ and $\Sigma_m^{(l)}$ cannot be joined at $g_{s,s'}^{l,\pm}$. Modifications to the junction rules induced by the existence of the exotic resonant-state poles have to be introduced. These modifications are given in Sec. II C.

Taking into account the S-matrix property $S_l(k,g)=S_l^*(-k^*,g^*)$, where * means complex conjugation, only the junctions of the sheets at the branch points whose images are situated in the fourth quadrant in the k plane will be given. The junctions at the branch points having the images symmetrically distributed with respect to the imaginary k axis can easily be deduced by using the above symmetry property of the S-matrix elements. At the branch points having images in the fourth quadrant of the k plane, the sheets $\Sigma_n^{(l)}$ and $\Sigma_m^{(l)}$ with $n,m>0$ for even l and with $n,m\geqslant 0$ for odd l, having the images $\Sigma_n'^{(l)}$ and $\Sigma_m'^{(l)}$ in the half-plane Re $k\geqslant 0$, are joined [1].

A. Junction rules at $g_{s,s'}^{l,\pm}$ with Re $k(g_{s,s'}^{l,\pm})>0$

In Fig. 2 the junctions between various Riemann sheets at the branch points with Re $k(g_{s,s'}^{l,\pm})>0$ are presented for various values of the orbital angular momentum l. The label n or m of each sheet is indicated by the number given at the left and right ends of the picture. Let $r=(l-1)/2$, $t=1$ for odd l, and $r=l/2$, $t=2$ for even $l>0$. Then (1) at the branch points $g_{s,p}^{l,-}$ $(p=t,t+1,\ldots,r)$ the sheet $\Sigma_{s+p-2}^{(l)}$ is joined to the sheet $\Sigma_{s+p-1}^{(l)}$, and (2) at the branch points $g_{s,p}^{l,+}$ $(p=t,t+1,\ldots,r+1)$ the sheet $\Sigma_{p-1}^{(l)}$ is joined to the sheet $\Sigma_{s+p-1}^{(l)}$. Here $s=1,2,\ldots$. The rules (1) and (2) for the junction of the sheets $\Sigma_n^{(l)}$ and $\Sigma_m^{(l)}$ at a branch point $g_{s,s'}^{l,\pm}$ are valid, provided that the pole corresponding to the potential strength value $g_{s,s'}^{l,\pm}$ is not an exotic resonant-state pole on both sheet images $\Sigma_n'^{(l)}$ and $\Sigma_m'^{(l)}$ (see for example, the cases $l=1,2,3,$ and 4 in Fig. 2). The modifications to the rules (1) and (2) induced by the existence of the exotic resonant-state poles on some Riemann sheets will be given in Sec. II C.

B. Junction rules at $g_{s,s'}^{l,\pm}$ with Re $k(g_{s,s'}^{l,\pm})=0$

A special case is that of the branch points $g_{s,1}^{l,\pm}$ for even l, having the images on the negative imaginary k axis. For even l at the branch points $g_{s,1}^{l,\pm}$, the junctions between the sheets with k-plane images in the half plane Re $k\leqslant 0$ and the sheets with the images in the half plane Re $k\geqslant 0$ occur. Due to this in the case of even l the junctions at the branch points $g_{s,1}^{l,\pm}$ are governed by rules that differ from the rules (1) and (2).

TABLE I. The branch points $g_{s,s'}^{l,\pm}$ whose k-plane images $\kappa_{s'}^{l,\pm}$ are situated in the fourth quadrant, including the negative k axis, in the cases $l=0-8$ for a rectangular potential. By $\kappa_{0,s}^{l,-}$ and $\kappa_{0,s}^{l,+}$ the zeros of the spherical Bessel function $j_{l-1}(z)$ and $j_{l+1}(z)$, respectively, are denoted. $\kappa_{s'}^{l,-}$ $(s'=1,\ldots,m)$, $m=(l-1)/2$ for odd $l>1$ and $m=l/2$ for even $l>0$ stand for the zeros of the spherical Hankel function of the first kind, $h_{l-1}^{(1)}(z)$, situated in the fourth quadrant of the k plane and on the imaginary k axis. $\kappa_{s'}^{l,+}$ $(s'=1,\ldots,m)$, $m=(l+1)/2$ for odd l and $m=l/2+1$ for even l, respectively, stand for the zeros of $h_{l+1}^{(1)}(z)$. In the present table only the first three branch points $g_{s,s'}^{l,\pm}$ for each value of s' are presented, i.e., the label s is limited to $s=1$, 2, and 3.

s'	s	$\kappa_{0,s}^{0,+}$	$\kappa_{s'}^{0,+}$	$g_{s,s'}^{0,+}$
1	1	4.493	$-i$	21.191
1	2	7.725	$-i$	60.679
1	3	10.904	$-i$	119.897
s'	s	$\kappa_{0,s}^{1,+}$	$\kappa_{s'}^{1,+}$	$g_{s,s'}^{1,+}$
1	1	5.763	$0.866-i1.500$	$34.717+i2.598$
1	2	9.095	$0.866-i1.500$	$84.219+i2.598$
1	3	12.323	$0.866-i1.500$	$153.355+i2.598$
s'	s	$\kappa_{0,s}^{2,-}$	$\kappa_{s'}^{2,-}$	$g_{s,s'}^{2,-}$
1	1	4.493	$-1.000i$	21.191
1	2	7.725	$-1.000i$	60.679
1	3	10.904	$-1.000i$	119.897
s'	s	$\kappa_{0,s}^{2,+}$	$\kappa_{s'}^{2,+}$	$g_{s,s'}^{2,+}$
1	1	6.988	$-2.322i$	54.224
1	2	10.417	$-2.322i$	113.909
1	3	13.698	$-2.322i$	193.028
2	1	6.988	$1.754-i1.839$	$49.135+i6.452$
2	2	10.417	$1.754-i1.839$	$108.820+i6.452$
2	3	13.698	$1.754-i1.839$	$187.940+i6.452$
s'	s	$\kappa_{0,s}^{3,-}$	$\kappa_{s'}^{3,-}$	$g_{s,s'}^{3,-}$
1	1	5.763	$0.866-i1.500$	$34.717+i2.598$
1	2	9.095	$0.866-i1.500$	$84.219+i2.598$
1	3	12.323	$0.866-i1.500$	$153.355+i2.598$
s'	s	$\kappa_{0,s}^{3,+}$	$\kappa_{s'}^{3,+}$	$g_{s,s'}^{3,+}$
1	1	8.183	$0.867-i2.896$	$74.590+i5.023$
1	2	11.705	$0.867-i2.896$	$144.641+i5.023$
1	3	15.040	$0.867-i2.896$	$233.827+i5.023$
2	1	8.183	$2.657-i2.104$	$64.319+i11.181$
2	2	11.705	$2.657-i2.104$	$134.368+i11.181$
2	3	15.040	$2.657-i2.104$	$223.556+i11.181$
s'	s	$\kappa_{0,s}^{4,-}$	$\kappa_{s'}^{4,-}$	$g_{s,s'}^{4,-}$
1	1	6.988	$-2.322i$	54.224
1	2	10.417	$-2.322i$	113.909
1	3	13.698	$-2.322i$	193.028
2	1	6.988	$1.754-i1.839$	$49.135+i6.452$
2	2	10.417	$1.754-i1.839$	$108.820+i6.452$
2	3	13.698	$1.754-i1.839$	$187.940+i6.452$
s'	s	$\kappa_{0,s}^{4,+}$	$\kappa_{s'}^{4,+}$	$g_{s,s'}^{4,+}$
1	1	9.356	$-3.647i$	100.830
1	2	12.967	$-3.647i$	181.430
1	3	16.355	$-3.647i$	280.775
2	1	9.356	$1.743-i3.352$	$95.730+i11.683$

TABLE I. (*Continued*).

s'	s	$\kappa_{0,s}^{4,+}$	$\kappa_{s'}^{4,+}$	$g_{s,s'}^{4,+}$
2	2	12.967	$1.743-i3.352$	$176.330+i11.683$
2	3	16.355	$1.743-i3.352$	$275.675+i11.683$
3	1	9.356	$3.571-i2.325$	$80.183+i16.603$
3	2	12.967	$3.571-i2.325$	$160.783+i16.603$
3	3	16.355	$3.571-i2.325$	$260.128+i16.603$
s'	s	$\kappa_{0,s}^{5,-}$	$\kappa_{s'}^{5,-}$	$g_{s,s'}^{5,-}$
1	1	8.183	$0.867-i2.896$	$74.590+i5.023$
1	2	11.705	$0.867-i2.896$	$144.641+i5.023$
1	3	15.040	$0.867-i2.896$	$233.827+i5.023$
2	1	8.183	$2.657-i2.104$	$64.319+i11.181$
2	2	11.705	$2.657-i2.104$	$134.368+i11.181$
2	3	15.040	$2.657-i2.104$	$223.556+i11.181$
s'	s	$\kappa_{0,s}^{5,+}$	$\kappa_{s'}^{5,+}$	$g_{s,s'}^{5,+}$
1	1	10.513	$0.868-i4.248$	$127.816+i7.371$
1	2	14.207	$0.868-i4.248$	$219.146+i7.371$
1	3	17.648	$0.868-i4.248$	$328.747+i7.371$
2	1	10.513	$2.626-i3.736$	$117.578+i19.622$
2	2	14.207	$2.626-i3.736$	$208.908+i19.622$
2	3	17.648	$2.626-i3.736$	$318.509+i19.622$
3	1	10.513	$4.493-i2.516$	$96.666+i22.606$
3	2	14.207	$4.493-i2.516$	$187.996+i22.606$
3	3	17.648	$4.493-i2.516$	$297.597+i22.606$
s'	s	$\kappa_{0,s}^{6,-}$	$\kappa_{s'}^{6,-}$	$g_{s,s'}^{6,-}$
1	1	9.356	$-3.647i$	100.830
1	2	12.967	$-3.647i$	181.430
1	3	16.355	$-3.647i$	280.775
2	1	9.356	$1.743-i3.352$	$95.730+i11.683$
2	2	12.967	$1.743-i3.352$	$176.330+i11.683$
2	3	16.355	$1.743-i3.352$	$275.675+i11.683$
3	1	9.356	$3.571-i2.325$	$80.183+i16.603$
3	2	12.967	$3.571-i2.325$	$160.783+i16.603$
3	3	16.355	$3.571-i2.325$	$260.128+i16.603$
s'	s	$\kappa_{0,s}^{6,+}$	$\kappa_{s'}^{6,+}$	$g_{s,s'}^{6,+}$
1	1	11.657	$-4.972i$	160.61
1	2	15.431	$-4.972i$	262.84
1	3	18.923	$-4.972i$	382.80
2	1	11.657	$1.739-i4.758$	$155.503+i16.552$
2	2	15.431	$1.739-i4.758$	$257.741+i16.552$
2	3	18.923	$1.739-i4.758$	$377.696+i16.552$
3	1	11.657	$3.517-i4.070$	$140.082+i28.631$
3	2	15.431	$3.517-i4.070$	$242.320+i28.631$
3	3	18.923	$3.517-i4.070$	$362.275+i28.631$
4	1	11.657	$5.421-i2.686$	$113.715+i29.116$
4	2	15.431	$5.421-i2.686$	$215.954+i29.116$
4	3	18.923	$5.421-i2.686$	$335.909+i29.116$
s'	s	$\kappa_{0,s}^{7,-}$	$\kappa_{s'}^{7,-}$	$g_{s,s'}^{7,-}$
1	1	10.513	$0.868-i4.248$	$127.816+i7.371$
1	2	14.207	$0.868-i4.248$	$219.146+i7.371$

TABLE I. (*Continued*).

s'	s	$\kappa_{0,s}^{7,-}$	$\kappa_{s'}^{7,-}$	$g_{s,s'}^{7,-}$
1	3	17.648	$0.868-i4.248$	$328.747+i7.371$
2	1	10.513	$2.626-i3.736$	$117.578+i19.622$
2	2	14.207	$2.626-i3.736$	$208.908+i19.622$
2	3	17.648	$2.626-i3.736$	$318.509+i19.622$
3	1	10.513	$4.493-i2.516$	$96.666+i22.606$
3	2	14.207	$4.493-i2.516$	$187.996+i22.606$
3	3	17.648	$4.493-i2.516$	$297.597+i22.606$
s'	s	$\kappa_{0,s}^{7,+}$	$\kappa_{s'}^{7,+}$	$g_{s,s'}^{7,+}$
1	1	12.791	$0.868-i5.588$	$194.076+i9.696$
1	2	16.641	$0.868-i5.588$	$307.395+i9.696$
1	3	20.182	$0.868-i5.588$	$437.804+i9.696$
2	1	12.791	$2.616-i5.205$	$183.850+i27.233$
2	2	16.641	$2.616-i5.205$	$297.169+i27.233$
2	3	20.182	$2.616-i5.205$	$427.578+i27.233$
3	1	12.791	$4.414-i4.368$	$163.199+i38.567$
3	2	16.641	$4.414-i4.368$	$276.518+i38.567$
3	3	20.182	$4.414-i4.368$	$406.927+i38.567$
4	1	12.791	$6.354-i2.839$	$131.29+i36.077$
4	2	16.641	$6.354-i2.839$	$244.611+i36.077$
4	3	20.182	$6.354-i2.839$	$375.020+i36.077$
s'	s	$\kappa_{0,s}^{8,-}$	$\kappa_{s'}^{8,-}$	$g_{s,s'}^{8,-}$
1	1	11.657	$-4.972i$	160.61
1	2	15.431	$-4.972i$	262.84
1	3	18.923	$-4.972i$	382.80
2	1	11.657	$1.739-i4.758$	$155.50+i16.552$
2	2	15.431	$1.739-i4.758$	$257.74+i16.552$
2	3	18.923	$1.739-i4.758$	$377.70+i16.552$
3	1	11.657	$3.517-i4.070$	$140.08+i28.631$
3	2	15.431	$3.517-i4.070$	$242.32+i28.631$
3	3	18.923	$3.517-i4.070$	$362.28+i28.631$
4	1	11.657	$5.421-i2.686$	$113.72+i29.116$
4	2	15.431	$5.421-i2.686$	$215.95+i29.116$
4	3	18.923	$5.421-i2.686$	$335.91+i29.116$
s'	s	$\kappa_{0,s}^{8,+}$	$\kappa_{s'}^{8,+}$	$g_{s,s'}^{8,+}$
1	1	13.916	$-6.297i$	233.30
1	2	17.839	$-6.297i$	357.87
1	3	21.428	$-6.297i$	498.83
2	1	13.916	$1.738-i6.129$	$228.20+i21.304$
2	2	17.839	$1.738-i6.129$	$352.77+i21.304$
2	3	21.428	$1.738-i6.129$	$493.73+i21.304$
3	1	13.916	$3.498-i5.604$	$212.82+i39.210$
3	2	17.839	$3.498-i5.604$	$337.39+i39.210$
3	3	21.428	$3.498-i5.604$	$478.35+i39.210$
4	1	13.916	$5.317-i4.638$	$186.89+i49.328$
4	2	17.839	$5.317-i4.638$	$311.46+i49.328$
4	3	21.428	$5.317-i4.638$	$452.42+i49.328$
5	1	13.916	$7.291-i2.979$	$149.36+i43.446$
5	2	17.839	$7.291-i2.979$	$273.93+i43.446$
5	3	21.428	$7.291-i2.979$	$414.89+i43.446$

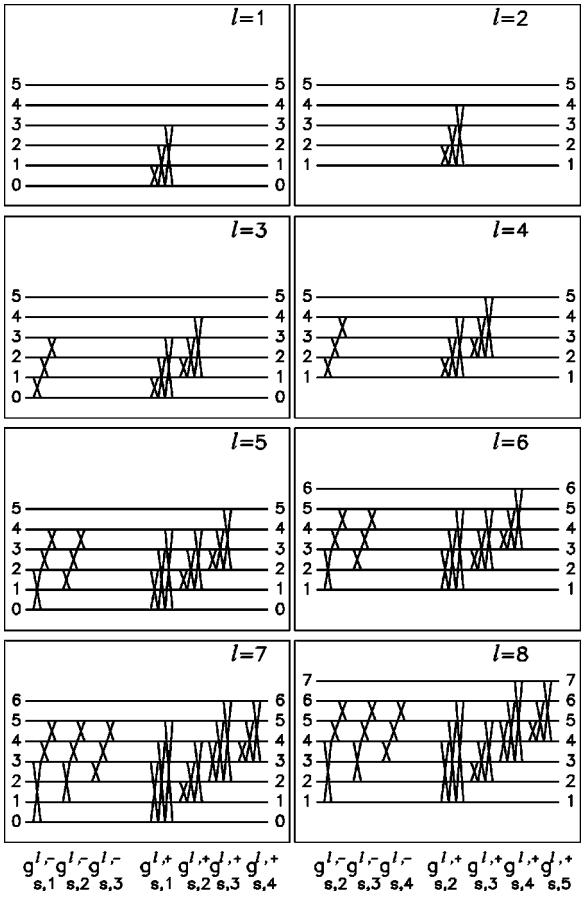

FIG. 2. Schematical representation of the junctions of the sheets $\Sigma_n^{(l)}$ and $\Sigma_m^{(l)}$, for a central rectangular potential with $l=1-8$ at the branch points $g_{s,s'}^{l,-}$ with $s=1$, 2, and 3 and $s'=t,t+1,\ldots,r$ and at the branch points $g_{s,s'}^{l,+}$ with $s=1$, 2, and 3 and $s'=t,t+1,\ldots,r+1$, where $r=(l-1)/2$, $t=1$ for odd l and $r=l/2$, $t=2$ for even l. The label n or m of each sheet is indicated by the number given at the left and right ends of the picture. These junctions have been established by the Riemann sheet analysis.

The junctions for even l at the branch points $g_{s,1}^{l,\pm}$ with $s=1,2$, and 3 are shown in Fig. 3.

1. Case $l=0$

In the case $l=0$ there is a single set of branch points, namely, $g_{s,1}^{0,+}$, whose image in the k plane is situated on the imaginary k axis at $k=\kappa_{s'}^{0,+}=-i$. The analysis of the Riemann surface $R_g^{(0)}$ shows that at $g_{s,1}^{0,+}$ the sheet $\Sigma_0^{(0)}$ cannot be joined to any other sheet of $R_g^{(0)}$. This means that the potential strength variation does not induce any jump between the ground state (0,0) and the other states $(0,n)$ of the system. At $g_{s,1}^{0,+}$ the sheets $\Sigma_s^{(0)}$ and $\Sigma_{-s}^{(0)}$ with $s>0$ are joined. In the case $l=0$, the following rules for the junctions of the Riemann sheets at the branch points can be extracted: (3) for $l=0$ the sheet $\Sigma_0^{(0)}$ is not joined to any other sheet, and (4) for $l=0$ at the branch points $g_{s,1}^{0,+}$ the sheet $\Sigma_s^{(0)}$ is joined to the sheet $\Sigma_{-s}^{(0)}$.

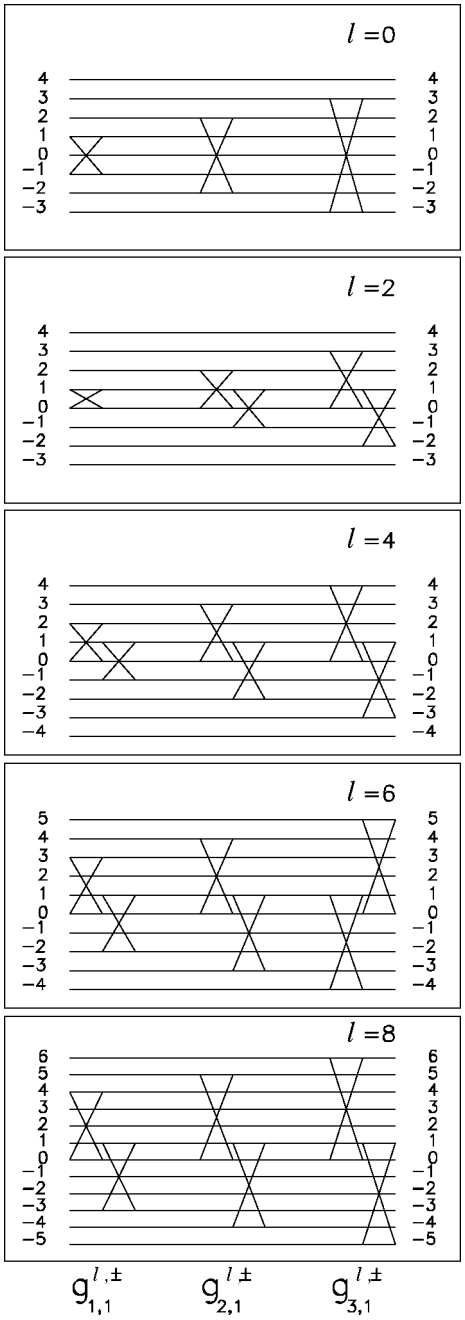

FIG. 3. Schematical representation of the junctions of the sheets $\Sigma_n^{(l)}$ and $\Sigma_m^{(l)}$, for a central rectangular potential with even $l=0-8$ at the branch points $g_{s,1}^{l,\pm}$ with $s=1$, 2, and 3. For $l=0$ there are only the branch points $g_{s,1}^{0,+}$. The label n or m of each sheet is indicated by the number given at the left and right ends of the picture. These junctions have been established by the analysis of the Riemann sheets.

2. Case $l>0$

By the analysis of the Riemann surfaces $R_g^{(l)}$ with even $l>0$ the rules for the junctions at $g_{s,1}^{l,\pm}$ have been deduced. It results that there are two pairs of sheets that are joined at each branch point $g_{s,1}^{l,\pm}$: (5) for even $l>0$ at the branch points $g_{s,1}^{l,\pm}$ the sheet $\Sigma_0^{(l)}$ is joined to the sheet $\Sigma_{l/2-1+s}^{(l)}$, and the sheet $\Sigma_1^{(l)}$ is joined to the sheet $\Sigma_{-l/2+2-s}^{(l)}$.

The rules (1–5) given above for the junction of various sheets define some selection rules for the jump from one sheet of the Riemann surface $R_g^{(l)}$ to some other sheet of the same surface. As it can be seen from Figs. 2 and 3, there are some sheets $\Sigma_n^{(l)}$ that are not joined to any other sheet at some $g_{s,s'}^{l,\pm}$, i.e., $g=g_{s,s'}^{l,\pm}$ is not a branch point for $\Sigma_n^{(l)}$. In this case the jump from $\Sigma_n^{(l)}$ to other sheet $\Sigma_m^{(l)}$ when the potential strength varies around $g_{s,s'}^{l,\pm}$ is forbidden.

As the k-plane images of the branch points are situated in the lower k half plane, the jumps occur only for potential strength variations around values for which the corresponding poles are resonant-state poles. There are not jumps between bound states induced by small potential strength variation.

C. Exceptions to the junction rules

As already mentioned, the junction rules that specify the labels n and m of the sheets that are joined at each branch point $g_{s,s'}^{l,\pm}$ are valid, provided that the pole corresponding to the potential strength $g_{s,s'}^{l,\pm}$ is not an exotic resonant-state pole on $\Sigma_m'^{(l)}$, where $m>n$. In the following, it will be shown that if for $g_{s,s'}^{l,\pm}$ there are exotic resonant-state poles on $\Sigma_n'^{(l)}$ and $\Sigma_m'^{(l)}$, where $m>n$, then the potential strength value $g=g_{s,s'}^{l,\pm}$ cannot be a branch point for $\Sigma_m^{(l)}$. As a consequence, $\Sigma_n^{(l)}$ and $\Sigma_m^{(l)}$ cannot be joined at $g_{s,s'}^{l,\pm}$, even in the case when the junction rule (1) or (2) would require this. In order to explain why the existence of the exotic resonant-state poles corresponding to the potential strength value $g_{s,s'}^{l,\pm}$ on both $\Sigma_n'^{(l)}$ and $\Sigma_m'^{(l)}$ leads to an exception to the junction rule at $g_{s,s'}^{l,\pm}$, in the following the main properties of the exotic resonant-state poles are outlined.

In Ref. [1] it was shown that for each $l\geqslant 1$ there are resonant-state poles for absorptive potential ($\mathrm{Im}\, g>0$) that do not become bound- or virtual-state poles as the potential strength g increases. Due to their unusual behavior these poles have been called "exotic resonant-state poles." In the fourth quadrant of the k plane of the sheet images $\Sigma_n'^{(l)}$, where $n=1,2,\ldots,l/2$ for even $l\geqslant 2$ and $n=0,1,2,\ldots,(l-1)/2$ for odd l, there are bound regions where the exotic resonant-state poles for absorptive potential are located. When the strength of the potential increases to infinity, the exotic resonant-state pole remains inside a certain bound region of the k plane. We remind that the label n of the Riemann sheets is the number which counts the poles as they occur at $g\to 0$ [see Eq. (3.17) of Ref. [1]].

The border of each bound region of the k plane, where an exotic resonant-state pole of the S-matrix element S_l is situated, lies on a pair of points: an attractor $\mathcal{K}_i^{(l)}$ which is a zero of the spherical Hankel functions of the first kind, $h_l^{(1)}(z)$, and the k-plane image of a branch point $k(g_{s,s'}^{l,\pm})$, which is a zero of the spherical Hankel functions of the first kind, $h_{l\pm1}^{(1)}(z)$. In Ref. [1] it was shown that $\mathcal{K}_i^{(l)}$ act as attractors for the exotic resonant-state poles; i.e., as $g\to\infty$, the exotic resonant-state pole tends to an attractor. On each of the sheet images $\Sigma_n'^{(l)}$, $n=1,2,\ldots,(l/2-1)$ for even $l>2$ and $n=0,1,\ldots,(l-3)/2$ for odd $l>1$, there are two such bound regions in the fourth quadrant of the k plane where the exotic poles are located. On the sheet image $\Sigma_n'^{(l)}$, with $n=l/2$ for even $l>0$ and $n=(l-1)/2$ for odd l, there is only a bound region of the k plane in the fourth quadrant of the k plane where the exotic poles are located. With the notation shown in Figs. 1(a) and 1(b), the analysis of the Riemann sheets on a large range of l values ($l=0$–8) allows us to draw the following conclusions concerning the localization of the bound regions in the k plane where the exotic resonant state poles are located: The bound region on $\Sigma_n'^{(l)}$, $n=l/2$ for even $l>0$ and $n=(l-1)/2$ for odd l, lies on $\mathcal{K}_n^{(l)}$ and on $k(g_{s,n+1}^{l,+})$. On the sheet images $\Sigma_n'^{(l)}$, $n=1,2,\ldots,(l/2-1)$ for even $l>2$ and $n=0,1,\ldots,(l-3)/2$ for odd $l>1$, there is a bound region that lies on $\mathcal{K}_n^{(l)}$ and $k(g_{s,n+1}^{l,+})$ and another bound region that lies on $\mathcal{K}_{n+1}^{(l)}$ and $k(g_{s,n+1}^{l,-})$.

On all the other sheet images [$n>(l-1)/2$ for odd l and $n>l/2$ for even $l\neq 0$] there are only usual resonant-state poles, i.e., poles that move towards the imaginary k axis as the strength of the potential well increases and become bound- or virtual-state poles for a sufficiently deep potential well.

The borders of a given sheet are made of the edges of the cuts taken along the branch points with the same imaginary part and a large radius circle that joins the cuts. The cuts that are boundaries of a given sheet $\Sigma_n^{(l)}$ determine some threshold values for the imaginary part of the complex potential strength g. For a given potential strength $g\in\Sigma_n^{(l)}$, the corresponding pole $k=k^{(l)}(g)$ on the sheet image $\Sigma_n'^{(l)}$ belongs to the usual or exotic class of resonant-state poles. This depends on the sheet to which the given g belongs and on the value of the absorption $\mathrm{Im}\, g>0$ with respect to the thresholds on that sheet. The situation is illustrated in Fig. 4(a) for even l and Fig. 4(b) for odd l. The exotic poles occur when the absorption of the potential on the given sheet is located in the corresponding region indicated by the hatching. There are exotic resonant-state poles for a strong ($\mathrm{Im}\, g>\mathrm{Im}\, g_{s,s'}^{l,+}$) or weak absorption ($\mathrm{Im}\, g<\mathrm{Im}\, g_{s,s'}^{l,-}$) potential. The strong absorption is related to the branch points whose k-plane images correspond to the zeros of $h_{l+1}^{(1)}(z)$, and the weak absorption is related to the branch points whose k-plane images correspond to the zeros of $h_{l-1}^{(1)}(z)$.

Let $\mathrm{Im}\, g_{s,p+1}^{l,\pm}$ be the absorption thresholds for the occurrence of the exotic resonant-state poles on the Riemann sheet image $\Sigma_p'^{(l)}$. Taking into account that the exotic resonant-state poles for a given l could occur only on the sheets with the labels $n=1,2,\ldots,l/2$ for even $l>0$ and $n=0,1,\ldots,(l-1)/2$ for odd l, and that the occurrence of an exotic resonant-state pole on $\Sigma_p'^{(l)}$ is determined by the absorption thresholds $\mathrm{Im}\, g_{s,p+1}^{l,\pm}$ on the corresponding Riemann sheet, the exception to the junction rule can be expressed as follows:

If for $g=g_{s,p+1}^{l,\pm}$, which defines the threshold for the absorption window on the sheet $\Sigma_p^{(l)}$, there is an exotic resonant-state pole on the Riemann sheet image $\Sigma_m'^{(l)}$ with $m>p$, i.e., if $\mathrm{Im}\, g_{s,p+1}^{l,\pm}=\mathrm{Im}\, g>\mathrm{Im}\, g_{s,m+1}^{l,+}$ or $\mathrm{Im}\, g_{s,p+1}^{l,\pm}=\mathrm{Im}\, g<\mathrm{Im}\, g_{s,m+1}^{l,-}$, then the potential strength value g

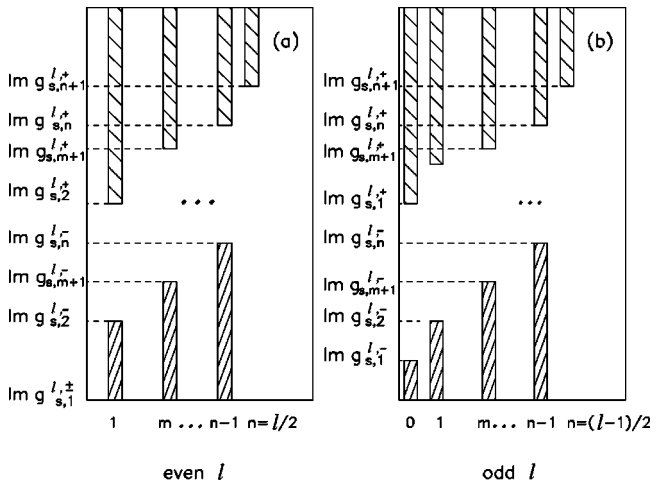

FIG. 4. Panels (a) and (b) give a schematic illustration of the absorption windows related to the imaginary parts of the branch points for a given $l \geqslant 1$. For even l we have $\mathrm{Im}\, g_{s,1}^{l,\pm}=0$. There are $l/2-1$ weak absorption windows ($\mathrm{Im}\, g<\mathrm{Im}\, g_{s,s'}^{l,-}$) for even l and $(l-1)/2$ weak absorption windows for odd l. There are $l/2$ strong absorption windows ($\mathrm{Im}\, g>\mathrm{Im}\, g_{s,s'}^{l,+}$) for even l and $(l+1)/2$ strong absorption windows for odd l. The label of the Riemann sheets where these absorption windows are situated is indicated on the abscissa.

$=g_{s,p+1}^{l,\pm}$ is not a branch point for the Riemann sheet $\Sigma_m^{(l)}$. Consequently, at $g=g_{s,p+1}^{l,\pm}$ the sheet $\Sigma_m^{(l)}$ cannot be joined to any other sheet.

Indeed, if it were an exotic pole on $\Sigma_m'^{(l)}$, this exotic pole would remain inside its own bound region that lies on an attractor, $\mathcal{K}_m^{(l)}$ or $\mathcal{K}_{m+1}^{(l)}$, which is a zero of $h_l^{(1)}(z)$ and on the k-plane image of the branch point $g_{s,m+1}^{l,\pm}$, and therefore it would be placed in some other region of the k plane as compared to the k-plane image of $g=g_{s,p+1}^{l,\pm}$, which is a zero of $h_{l\pm1}^{(1)}(z)$. For example, let us suppose that in the case $l=5$ the potential strength takes the value $g=g_{1,1}^{5,-}=74.590+i5.023$. As $\mathrm{Im}\, g_{s,1}^{5,-}<\mathrm{Im}\, g_{s,2}^{5,-}=11.181$, for $g=g_{1,1}^{5,-}$ the pole on $\Sigma_1'^{(5)}$ will be an exotic pole and will be situated in a bound region of the k plane that lies on the image of the branch point $g_{s,2}^{5,-}$ [i.e., $\kappa_2^{5,-}=k(g_{s,2}^{5,-})=2.657-i2.104$] and on the attractor $\mathcal{K}_2^{(5)}=3.571-i2.325$. This pole cannot be brought in the neighborhood of the k-plane image of $g_{s,1}^{5,-}$ [i.e., $\kappa_1^{5,-}=k(g_{s,1}^{5,-})=0.867-i2.896$], does not matter how much the potential strength is varied. Consequently, $g=g_{s,1}^{5,-}$ are not branch points for $\Sigma_1^{(5)}$. That is why the jump at $g_{1,1}^{5,-}$ between the sheets $\Sigma_0^{(5)}$ to $\Sigma_1^{(5)}$ is forbidden. Correspondingly, at $g_{1,1}^{5,-}$ the jump between the associated states is forbidden, i.e., $(5,0)\Leftrightarrow(5,1)$ is forbidden. Instead of this, at $g_{1,1}^{5,-}$ the sheet $\Sigma_0^{(5)}$ is joined to the next sheet, i.e., to $\Sigma_2^{(5)}$, and a small variation of the potential strength around $g_{1,1}^{5,-}$ can induce the jump $(5,0)\Leftrightarrow(5,2)$.

In case the pole corresponding to $g_{s,s'}^{l,\pm}$ is an exotic resonant-state pole on both sheet images $\Sigma_n^{(l)}$ and $\Sigma_m^{(l)}$, the junction rules (1) and (2) have to be modified as follows:

If the pole corresponding to $g=g_{1,p}^{l,-}$ is an exotic resonant-state pole on $\Sigma_{p-1}'^{(l)}$ and $\Sigma_p'^{(l)}$, then $g_{1,p}^{l,-}$ is not a branch point

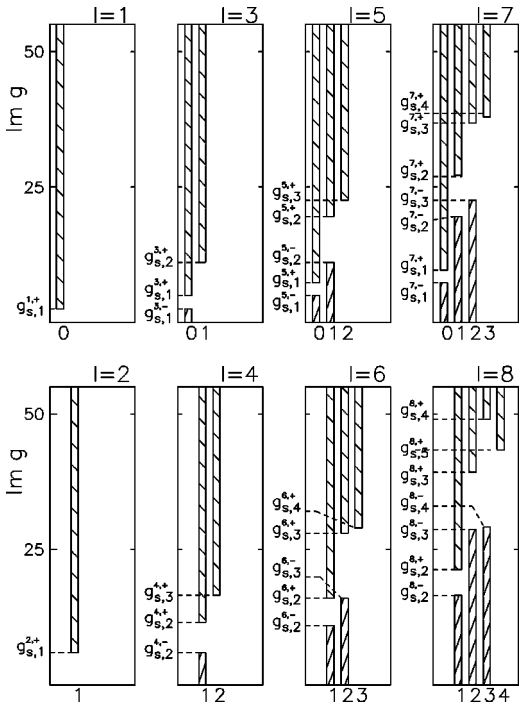

FIG. 5. The figure indicates by hatching the absorption windows for the exotic resonant-state poles in the fourth quadrant of various Riemann sheet images in the k plane in the case $l=1-8$. The labels of the sheets for each l are indicated on the abscissa.

for $\Sigma_p^{(l)}$. Consequently, $\Sigma_{p-1}^{(l)}$ cannot be joined at $g_{1,p}^{l,-}$ to $\Sigma_p^{(l)}$, as the rule (1) would require, but it will be joined to the sheet $\Sigma_{p+1}^{(l)}$, provided that the pole on $\Sigma_{p+1}'^{(l)}$ is not an exotic resonant-state pole, otherwise $\Sigma_{p-1}^{(l)}$ will be joined to $\Sigma_{p+2}^{(l)}$, etc. Once the junction at $g_{1,p}^{l,-}$ is established, the junctions at $g_{s,p}^{l,-}$ $(s=2,3,4,\ldots)$ are determined as follows: Let us suppose that at $g_{1,p}^{l,-}$ the sheets $\Sigma_{p-1}^{(l)}$ and $\Sigma_{p+q}^{(l)}$ are joined, then at $g_{s,p}^{l,-}$ the sheets $\Sigma_{s+p+q-2}^{(l)}$ and $\Sigma_{s+p+q-1}^{(l)}$ are joined.

Similarly, if the pole corresponding to $g=g_{s,p}^{l,+}$ is an exotic resonant-state pole on $\Sigma_{p-1}'^{(l)}$ and $\Sigma_{s+p-1}'^{(l)}$, then $g_{s,p}^{l,+}$ is not a branch point for $\Sigma_{s+p-1}^{(l)}$. Consequently, $\Sigma_{p-1}^{(l)}$ cannot be joined at $g_{s,p}^{l,+}$ to $\Sigma_{s+p-1}^{(l)}$, as the rule (2) would require, but it will be joined to $\Sigma_{s+p}^{(l)}$, provided that the pole corresponding to $g_{s,p}^{l,+}$ is not an exotic resonant-state pole on $\Sigma_{s+p}'^{(l)}$, otherwise $\Sigma_{p-1}^{(l)}$ will be joined to $\Sigma_{s+p+1}^{(l)}$, etc.

In the following, a simple method to identify the forbidden jumps will be given. It is based on the calculation of the thresholds for the absorption windows that determine the existence of the exotic resonant-state poles on some sheets. From Fig. 5 it is easy to understand the exceptions to the junction rules (1) and (2). Figure 5 gives the absorption windows for the existence of the exotic resonant-state poles on various Riemann sheet images in the k plane in the case $l=1-8$. Let $g_{s,p}^{l,\pm}$ be the potential strength value at which the sheet $\Sigma_n^{(l)}$ should be joined to other sheet, according to the junction rules. From Fig. 5 one can see which are the sheet images $\Sigma_m'^{(l)}$ on which there are exotic resonant-state poles corresponding to this potential strength value. In this way the forbidden jumps $(l,n)\Leftrightarrow(l,m)$ at $g_{s,s'}^{j,\pm}$ can be identified, and

therefore one can see the cases where the modified junction rules have to be used. For example, for $l=7$ the sheet $\Sigma_0^{(7)}$ should be joined, according to the rules (1) and (2), to the sheet $\Sigma_1^{(7)}$ at $g_{1,1}^{7,\pm}$. However, $g_{s,1}^{7,\pm}$ are not branch points for $\Sigma_1^{(7)}$. Indeed, as it can be seen from Fig. 5, the pole on $\Sigma_1'^{(7)}$ that corresponds to $g=g_{s,1}^{7,\pm}$ is an exotic pole, because $\mathrm{Im}\, g_{s,1}^{7,\pm}=\mathrm{Im}\, g<\mathrm{Im}\, g_{s,2}^{7,-}$. This pole remains in the bound region of the k plane that lies on the image of $g_{s,2}^{7,-}$ on $\Sigma_1'^{(7)}$ ($\kappa_2^{7,-}=2.626-i3.736$) and on the stable point $\mathcal{K}_2^{(7)}=3.517-i4.070$. This exotic pole cannot be brought near the image of $g_{s,1}^{7,+}$ ($\kappa_1^{7,+}=0.868-i5.588$) or near the image of $g_{s,1}^{7,-}$ ($\kappa_1^{7,-}=0.868-i4.248$). Consequently, the sheet $\Sigma_0^{(7)}$ cannot be joined with the sheet $\Sigma_1^{(7)}$ at $g_{1,1}^{7,\pm}$. For a similar reason the sheet $\Sigma_0^{(7)}$ cannot be joined with the sheet $\Sigma_2^{(7)}$ at $g_{1,1}^{7,\pm}$. Consequently, the jumps $(7,0)\Leftrightarrow(7,1)$ and $(7,0)\Leftrightarrow(7,2)$ are forbidden. Similarly, at $g_{1,2}^{7,-}$ the sheet $\Sigma_1^{(7)}$ cannot be joined with the sheet $\Sigma_2^{(7)}$ and the jump $(7,1)\Leftrightarrow(7,2)$ is forbidden. For $l=8$ it can be seen that at $g_{1,2}^{8,\pm}$ the sheet $\Sigma_1^{(8)}$ cannot be joined either with the sheet $\Sigma_2^{(8)}$ or with $\Sigma_3^{(8)}$. At $g_{1,3}^{8,-}$ the sheet $\Sigma_2^{(8)}$ cannot be joined with the sheet $\Sigma_3^{(8)}$. At $g_{s,4}^{8,+}$ the sheet $\Sigma_3^{(8)}$ cannot be joined with the sheet $\Sigma_4^{(8)}$. Consequently, for $l=8$ the jumps $(8,1)\Leftrightarrow(8,2)$ and $(8,1)\Leftrightarrow(8,3)$ are forbidden. The jump $(8,2)\Leftrightarrow(8,3)$ is forbidden for the potential strength variation in the neighborhood of $g_{s,3}^{8,-}$, but it is allowed near $g_{s,3}^{8,+}$. Similarly, the jump $(8,3)\Leftrightarrow(8,4)$ is forbidden near $g_{s,4}^{8,+}$, but it is allowed near $g_{s,4}^{8,-}$.

By the simple calculation of the potential absorption windows that determine the occurrence of the exotic resonant-state poles on the corresponding Riemann sheet images, one can directly establish the jumps between the sheets for small potential strength variation around a branch point. As the exotic resonant-state poles occur on a small number of Riemann sheet images $\Sigma_n'^{(l)}$ [$n=1,2,\ldots,l/2$ for even $l>0$ and $n=0,1,\ldots,(l-1)/2$ for odd l], at a first sight it could seem that a general rule for the jumps, which includes the modifications mentioned above, would be possible. This is not true because the thresholds $\mathrm{Im}\, g_{s,s'}^{l,\pm}$ of the absorption windows that determine the occurrence of the exotic resonant-state poles on a given Riemann sheet image $\Sigma_n'^{(l)}$ do not depend monotonically on the label n of the sheets (see, e.g., the case $l=8$ in Fig. 5, where there is an inversion between $\mathrm{Im}\, g_{s,4}^{8,+}$ and $\mathrm{Im}\, g_{s,5}^{8,+}$; for larger values of l there are numerous inversions of this kind).

III. LOCAL DEGENERACY WITH RESPECT TO THE ORBITAL ANGULAR MOMENTUM

Besides the junctions between the sheets of a given Riemann surface $R_g^{(l)}$, discussed above, there are junctions between the sheets of the Riemann surfaces for different l. In Ref. [1] it was shown that the resonant levels for the rectangular central potential exhibit a local degeneracy with respect to the orbital angular momentum l. Let $g_{j,i}^{(l)}$ ($j=1,2,\ldots$) be the set of potential-well strengths for which there is a resonant state of angular momentum l corresponding to a pole k situated at an attractor $\mathcal{K}_i^{(l)}\in\Sigma_i'^{(l)}$. In Ref. [1] it was demonstrated that there are three sheets belonging to three distinct Riemann surfaces $R_g^{(l)}$, $R_g^{(l-1)}$, and $R_g^{(l+1)}$ that are joined at a given value of the potential strength from the set $g_{j,i}^{(l)}$. A careful analysis of the Riemann surfaces shows that at $g_{j,i}^{(l)}$, for which there is a pole at the attractor $\mathcal{K}_i^{(l)}\in\Sigma_i'^{(l)}$, the sheets $\Sigma_q^{(l-1)}$, $\Sigma_i^{(l)}$, and $\Sigma_q^{(l+1)}$ ($l>1$), where $q=j+i-1$ for even l and $q=j+i$ for odd l, are joined. Here $i=1,2,\ldots,l/2$ for even l and $i=1,2,\ldots,(l-1)/2$ for odd l. For odd l there is also an attractor $\mathcal{K}_0^{(l)}$ situated on the imaginary k axis of $\Sigma_0'^{(l)}$. This attractor is reached for a potential value in the set $g_{j,0}^{(l)}$, with $j=1,2,\ldots$. For $g=g_{j,0}^{(l)}$ (odd l) the sheets $\Sigma_0^{(l-1)}$, $\Sigma_0^{(l)}$, and $\Sigma_0^{(l+1)}$ are joined.

This means that a resonant level (l,i) with orbital angular momentum l, corresponding to a pole situated at an attractor $\mathcal{K}_i^{(l)}$, is degenerate with other resonant levels with orbital angular momenta $l-1$ and $l+1$. If the potential strength g varies around the value $g=g_{j,i}^{(l)}$, the position of the pole in the k plane and the corresponding level energy changes for all three partial waves $l-1,l,l+1$ with different rates of change. In Ref. [11] the derivative dk^2/dg that describes the rate of change of the pole position for the orbital angular momentum l with respect to the potential strength variation has been calculated,

$$\frac{dk^2}{dg}=-\frac{k^2+g}{g}\frac{h_l^{(1)}(k)}{h_{l-1}^{(1)}(k)h_{l+1}^{(1)}(k)}+\frac{k^2}{g}. \tag{4}$$

Let us suppose that the potential has a small variation around the value $g_{j,i}^{(l)}$ for which there is a pole at the attractor $\mathcal{K}_i^{(l)}$ on $\Sigma_i'^{(l)}$. For $k=\mathcal{K}_i^{(l)}$, where $\mathcal{K}_i^{(l)}$ is a zero of $h_l^{(1)}(k)$ (stable point), and for large g we obtain from Eq. (4) $dk^2/dg\to 0$, i.e., the pole for the orbital angular momentum l is stable with respect to the potential strength variation. For the same potential strength value $g_{j,i}^{(l)}$ there is a pole for $l-1$ and a pole for $l+1$, which are situated at the k-plane image of a branch point. By replacing $l\to l-1$ and $l\to l+1$ in Eq. (4), we obtain the rate of change of the pole position in the waves $l-1$ and $l+1$ for the potential strength varying around $g_{j,i}^{(l)}$. It results in $dk^2/dg\to\infty$, i.e., the position of the pole in the waves $l-1$ and $l+1$ is unstable with respect to the potential strength variation.

For example, for $g=g_{1,1}^{(2)}=34.717+i2.598$ there is a pole at the stable point $\mathcal{K}_1^{(2)}=0.866-i1.500$ on $\Sigma_1'^{(2)}$. For the same potential value there is also a pole at $\kappa_1^{1,+}=k(g_{s,1}^{1,+})=0.866-i1.500$ on $\Sigma_1'^{(1)}$ and a pole at $\kappa_1^{3,-}=k(g_{s,1}^{3,-})=0.866-i1.500$ on $\Sigma_1'^{(3)}$. The sheets $\Sigma_1^{(1)}$, $\Sigma_1^{(2)}$, and $\Sigma_1^{(3)}$ are joined at $g=g_{1,1}^{(2)}$. In Fig. 6 the derivative dk^2/dg is shown for $l=1,2,3$, with g taking values around the value $g=g_{1,1}^{(2)}$, for which on $\Sigma_1'^{(2)}$ the pole is situated at the attractor. One can see that for $l=2$ the derivative dk^2/dg has a small value with a minimum around $g=g_{1,1}^{(2)}$, while for $l=1$ and $l=3$ the derivative has a sharp change, with a maximum for this value of the potential. This means that in the wave $l=2$ the system reaches a stable equilibrium, while in the waves $l=1$ and $l=3$ the system is unstable in the neighborhood of $g=g_{1,1}^{(2)}$. The sharp change in the pole position for $l=1$ and $l=3$ induced by the potential strength variation

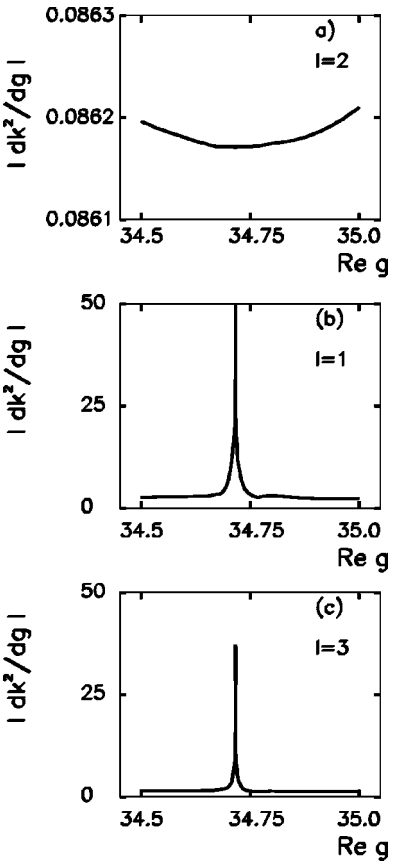

FIG. 6. The absolute value of the derivative dk^2/dg for three adjacent values of l ($l=1,2,3$) around the value of $g=g_{1,1}^{(2)}=34.717+i\,2.598$, for which there is an attractor on $\Sigma_1'^{(2)}$. Im g has been kept constant to the value Im $g=2.598$.

means that the degeneracy of the three waves at $g=g_{1,1}^{(2)}$ can easily be removed. At $g=g_{2,1}^{(2)}=84.219+i2.598$ there is a pole at $\kappa_1^{1,+}$ on $\Sigma_2'^{(1)}$ and a pole at $\kappa_1^{3,-}$ on $\Sigma_2'^{(3)}$, so that at $g=g_{2,1}^{(2)}$ the sheets $\Sigma_2^{(1)}$, $\Sigma_1^{(2)}$, and $\Sigma_2^{(3)}$ are joined. Similarly, at $g=g_{3,1}^{(2)}=153.355+i2.598$ there is a pole at $\kappa_1^{1,+}$ on $\Sigma_3'^{(1)}$ and a pole at $\kappa_1^{3,-}$ on $\Sigma_3'^{(3)}$, so that at $g=g_{2,1}^{(2)}$ the sheets $\Sigma_3^{(1)}$, $\Sigma_1^{(2)}$ and $\Sigma_3^{(3)}$ are joined.

Equation (4) shows that the derivative dk^2/dg becomes closer and closer to zero in the neighborhood of $g_{j,i}^{(l)}$ with increasing value of the potential strength from the set $g_{j,i}^{(l)}$. In other words, for a given l the stability of the system in the neighborhood of the attractor increases by increasing the depth of the potential well, g. This conclusion is illustrated in Fig. 7, where the derivative dk^2/dg for $l=2$ is shown as the potential varies in the neighborhood of $g_{1,1}^{(2)}$, $g_{2,1}^{(2)}$, and $g_{3,1}^{(2)}$, respectively. Equal lengths of the interval for Re g variation, centered on Re $g_{1,1}^{(2)}$, Re $g_{2,1}^{(2)}$, and Re $g_{3,1}^{(2)}$, respectively, have been taken. One can see that the curve dk^2/dg vs Re g is flatter and closer to zero with increasing $g_{j,i}^{(2)}$.

The degeneracy described above occurs for some particular values of the potential strength, i.e., it is a local degeneracy. Due to exact local degeneracy three angular momenta do contribute to the resonant cross section. This degeneration supports a new type of resonance in the cross section, which is associated to the cooperative contribution of three adjoint angular momenta.

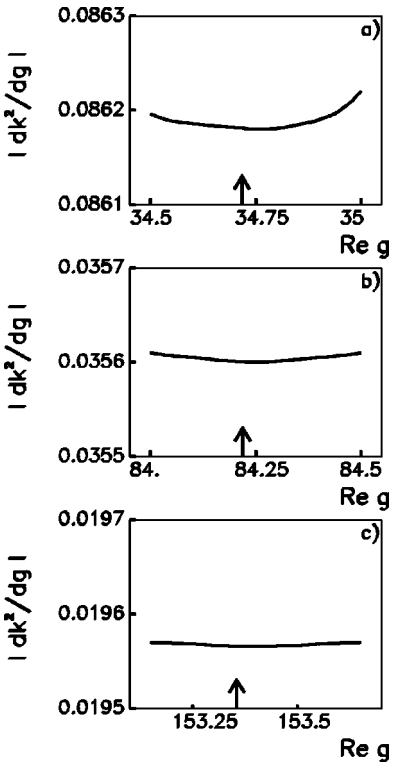

FIG. 7. The derivative dk^2/dg for $l=2$ in the neighborhood of three successive values of $g_{j,1}^{(2)}$ for which there is a pole near the attractor $\mathcal{K}_1^{(2)}$: $g_{1,1}^{(2)}=34.717+i2.598$, $g_{2,1}^{(2)}=84.219+i2.598$, and $g_{3,1}^{(2)}=153.355+i2.598$, respectively. By arrows Re $g_{j,1}^{(2)}$ is indicated. Im g has been kept constant to the value Im $g=2.598$.

The exact local degeneracy of three partial waves occurs also in the case when a Coulomb barrier for a point charge is added to the rectangular well potential Ref. [12]. In [11] the effect of the potential-well diffuseness on the pole positions was studied. It was shown that the attractor $\mathcal{K}_i^{(l)}$ is slightly shifted and that the poles in the waves $(l-1)$ and $(l+1)$ are shifted too, provided that the diffuseness is small. Consequently, for a diffuse edge well at $g_{j,i}^{(l)}$, for which there is a pole at the attractor $\mathcal{K}_i^{(l)}\in\Sigma_i'^{(l)}$, the levels $(l-1,q)$, (l,i), and $(l+1,q)$, where $q=j+i-1$ for even l and $q=j+i$ for odd l, are rather quasidegenerate than degenerate.

IV. CONCLUSIONS

The effects of the potential strength variation on the S-matrix poles are discussed in the framework of the Riemann surface approach to bound and resonant states.

By associating a sheet $\Sigma_n^{(l)}$ of the Riemann surface of the function $k^{(l)}(g)$ over the g plane and the corresponding k-plane image $\Sigma_n'^{(l)}$ to each state with the quantum numbers (l,n) the jump between the states (l,n) and (l,m), induced by a small potential strength variation around a branch point $g_{s,s'}^{l,\pm}$, is treated as the jump between the sheets $\Sigma_n^{(l)}$ and $\Sigma_m^{(l)}$.

The rules for the jumps between states with $\Delta l=0$, i.e., $(l,n)\Leftrightarrow(l,m)$, are established. In other words, the labels n and m of the sheets $\Sigma_n^{(l)}$ and $\Sigma_m^{(l)}$, and of the corresponding

k-plane images that are joined at a given branch point $g_{s,s'}^{l,\pm}$, are determined. The forbidden jumps can be identified by the calculation of the thresholds of the absorption windows for the potential, which determine the occurrence of the exotic resonant state poles on various Riemann sheet images $\Sigma_i'^{(l)}$. It is shown that if for a given $g_{s,s'}^{l,\pm}$ there are exotic resonant state poles on $\Sigma_n'^{(l)}$ and $\Sigma_m'^{(l)}$, where $m>n$, then the potential strength value $g_{s,s'}^{l,\pm}$ is not a branch point for $\Sigma_m^{(l)}$ and, consequently, $\Sigma_n^{(l)}$ and $\Sigma_m^{(l)}$ cannot be joined at $g_{s,s'}^{l,\pm}$, even in the case where the junction rules would require this. The modifications to the junction rules, induced by the existence of the exotic resonant-state poles, are given.

The local degeneracy of the energy levels for three partial waves $l-1$, l, and $l+1$ is generated by the potential strength variation around the value for which there is an attractor on a Riemann sheet for the orbital momentum l. For this potential value the system reaches a stable equilibrium in the wave l and is unstable in the waves $l-1$ and $l+1$.

[1] C. Grama, N. Grama, and I. Zamfirescu, Phys. Rev. A **61**, 032716 (2000).

[2] R. Seydel, *Practical Bifurcation and Stability Analysis. From Equilibrium to Chaos*, 2nd ed. (Springer-Verlag, New York, 1994).

[3] C. Grama, N. Grama, and I. Zamfirescu, Ann. Phys. (N.Y.) **232**, 243 (1994).

[4] E. Hernández, A. Jáuregui, and A. Mondragón, J. Phys. A **33**, 4507 (2000).

[5] E. Hernández and A. Mondragón, Phys. Lett. B **326**, 1 (1994).

[6] W. Vanroose, P. van Leuwen, F. Arickx, and J. Broeckhove, J. Phys. A **30**, 5543 (1997).

[7] N.J. Kylstra and C.J. Joachain, Europhys. Lett. **36**, 657 (1996); Phys. Rev. A **57**, 412 (1998).

[8] O. Latinne, N.J. Kylstra, M. Dörr, J. Purvis, M. Terao-Dunseath, C.J. Joachain, P.G. Burke, and C.J. Noble, Phys. Rev. Lett. **74**, 46 (1995).

[9] A. Cyr, O. Latinne, and P.G. Burke, J. Phys. B **30**, 659 (1997).

[10] H.A. Antosiewicz, in *Handbook of Mathematical Functions with Formulas, Graphs and Mathematical Tables*, edited by M. Abramovitz and I.A. Stegun, Natl. Bur. Stand. Applied Mathematics Series, 9th printing (U.S. GPO, Washington, D.C., 1970), p. 435.

[11] C. Grama, N. Grama, and I. Zamfirescu, Ann. Phys. (N.Y.) **218**, 346 (1992).

[12] C. Grama, N. Grama, and I. Zamfirescu, Europhys. Lett. **39**, 353 (1997).